EUROPEAN ORGANIZATION FOR NUCLEAR RESEARCH

ATLAS Internal Note
December 21, 1999

Single Top quark production via W-gluon fusion at LHC. Simulation with PYTHIA 5.7 Event generator.

A. Ahmedov[1)], **A.P. Cheplakov**[2)], **V.V. Kukhtin**[2)], **R. Mehdiyev**[1)*], **Z. Metreveli**[3)], **D. Salihagić**[4)]

Abstract

The electroweak production of single top quarks via so - called W - gluon fusion in proton-proton interactions at $\sqrt{s} = 14$ TeV has been studied. Single top quark production cross sections have been calculated. Simulations of the top quark production in W - gluon fusion process with further decay to $Wb \rightarrow l\nu b$ final state has been performed. The use of several kinematical distributions allowed to suppress background and to perform the reconstruction of the mass of the $e - \nu - jet$ system. At an integrated luminosity of $3 \times 10^4 pb^{-1}$, the signal-to-background ratio close to 5 is achived.

[1)] Institute of Physics, Azerbaijan Academy of Sciences, Baku, Azerbaijan.
[2)] Joint Institute for Nuclear Research, Dubna, Russian Federation.
[3)] Institute for High Energy Physics, Tbilisi State University, Georgia.
[4)] University of Montenegro, Podgorica, Montenegro.
[*)] Now at Université de Montréal, Montréal, Canada.

EUROPEAN ORGANIZATION FOR NUCLEAR RESEARCH

1 Introduction

The top quark discovery[1, 2] opened up a new and exciting area of physics. Within the limited statistics available the results, recently presented by the CDF and D0 experiments confirm the Standard Model (SM) predictions. However, a copious top production at LHC can bring many surprises.

Non-standard models, as an alternative to the SM, for the top quark production[3, 4], or decay[5] (or a combination of both[6]) have received a considerable attention.

The precise top quark mass reconstruction is an important parameter to understand the mechanism of particle mass generation.

The top quark mass determination is also of a high importance for many physics processes to be investigated at LHC.

Single top quarks are produced at hadron colliders mainly from a Wtb vertex, and thereby provide a direct probe of the Wtb coupling nature via the measurement of the Cabibbo-Kobayashi-Maskawa (CKM) matrix element, $|V_{tb}|$. This could be done, because the single top quark cross-section is directly related to the $|V_{tb}|$. Therefore a good signal-to-background ratio is needed to measure the cross section value with a high accuracy and improve the measurement of V_{tb}.

The top quark mixing with other flavors is very small, so that the CP violation in this process in the frame of the SM is negligible.

The ATLAS experiment sensitivity to many topics related to top quarks physics were presented in Physics Performance Technical Design Report (TDR)[21]. Our study was performed mainly during the preparation stage of the TDR and was partially presented there.

2 Electroweak single top quark production

The dominant subprocesses for the heavy quark production are low-order QCD quark-antiquark and gluon-gluon fusion mechanisms in the *s* - , *t* - , and *u* - channels:

- $q\overline{q} \rightarrow t\overline{t}$
- gg $\rightarrow t\overline{t}$

(pair productions), which yield large top quark samples, allowing detailed studies of many properties of top quarks production and decay.

However, the precise determination of the Wtb vertex properties and associated coupling strengths, will more likely be obtained from measurements of the electroweak production of single top quarks. Single top quarks production processes can be classified as following:

1. $pp \rightarrow t\overline{b} + X$ via *s* - channel W - boson
   - 1.1. $q\overline{q}^{'} \rightarrow t\overline{b}$
   - 1.2. $qg \rightarrow t\overline{b}\, q^{'}$
   - 1.3. $q\overline{q} \rightarrow t\overline{b}$ W
2. $pp \rightarrow tq + X$ via *t* - or *u* - channel W - boson
   - 2.1. $qb \rightarrow tq$
   - 2.2. $qb \rightarrow tqg$
   - 2.3. $qg \rightarrow tq\overline{q}$
   - 2.4. $bg \rightarrow tqg$
3. $pp \rightarrow tW^{-} + X$
   - 3.1. $bg \rightarrow tW$
   - 3.2. $bg \rightarrow tWg$
   - 3.3. $qq \rightarrow tW\overline{b}$
   - 3.4. $gg \rightarrow tW\overline{b}$
   - 3.5. $qb \rightarrow tWq$

The notation used: q is a light quark (u,d,s,c), X represents any additional final state particles from the pp interaction and q' denotes different quark's flavour.

Processes 1.2, 1.3, 2.2, 2.4, 3.2 usually are taken into account as radiative corrections.

The cross section values for all processes listed here are calculated in this paper (section 3).

For two diagrams (2.1 and 2.2), usually referred to as the "2-2" and "2-3" processes, shown in Fig. 1a) and Fig. 1b), respectively. Both diagrams refer to the same so-called "W-gluon fusion" [8] process. Since the W-gluon fusion process is the largest source of a single top quark production at LHC, with an expected cross-section of ~ 250 pb, it will be a source for it's physics sensitivity, as well as a serious background for other single top quark processes.

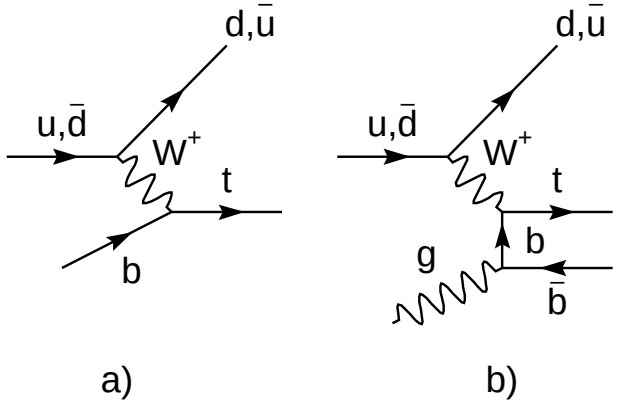

Figure 1: Feynman diagrams for the single top quark production processes - (W -gluon fusion): a) $qb \rightarrow tq'$, b) $qg \rightarrow tq'b$

As a background to the single top quark production, $t\bar{t}$ pair production and W-boson production accompanied by two and more jets have been considered in our study.

3 Cross section calculation

The following SM parameters were used in the cross-section calculations: M_W=81 GeV, M_Z=91 GeV, $sin^2\theta_W$=0.225, M_b=5 GeV, α =1/137, and CKM matrix elements V_{ud} =0.975 and V_{tb}=0.999.

The Λ_{QCD} scale parameter (for five quark flavors) has been chosen equal to 200 MeV.

For the cross-section calculations and various processes considered, following scale parameters have been used: $Q^2 = \hat{s}$ (process 1), $Q^2 = M_w^2$ (2 $\rightarrow$ 2 processes 2 and 3) and $Q^2 = M_t^2 + P_t^2$ (2 $\rightarrow$ 3 processes 2 and 3).

The cross-section were calculated taking into account Next-to-Leading Order (NLO) corrections (for processes 2 and 3 Leading Order (LO) corrections shown) , and reported, for various processes in Tables from 1 to 6[1)]

The total cross section for the production of the top quark in the subprocesses 1.1 and 1.2 is 7.6 pb; in the subprocesses 2.1 and 2.2 (W-g fusion) is 159.36 pb; and in the subprocesses 3.1 and 3.2 – 80.94 pb. The corresponding total cross-section for production of the $\bar{t}$ quark are: 2.84 pb, 98.02 pb, 80.34 pb for the same subprocesses.

[1)] the cross-section values presented are corresponding to the production of the top quark only.

Table 1: Process 1.1. $q\overline{q} \rightarrow t\overline{b}$.

Subprocess	$u\overline{d} \rightarrow t\overline{b}$	$q\overline{q} \rightarrow t\overline{b}$
σ (NLO) [pb]	2.91	2.91
σ (LO) [pb]	5.69	5.69

Table 2: Process 1.2 $qg \rightarrow t\overline{b}q$ (s-channel).

Subprocess	$ug \rightarrow t\overline{b}d$	$\overline{d}$g $\rightarrow t\overline{b}\overline{u}$	$qg \rightarrow t\overline{b}q$
σ(NLO) [pb]	1.17	0.24	1.41
σ(LO) [pb]	1.50	0.41	1.91

Table 3: Process 2.1 $qb \rightarrow tq$.

Subprocess type	$ub \rightarrow td$	$\overline{d}b \rightarrow t\overline{u}$	$qb \rightarrow tq$
σ [pb]	84.36	32.53	116.89

Table 4: Process 2.2 $qg \rightarrow t\overline{b}q$ (u-channel).

Subprocess	$ug \rightarrow td\overline{b}$	$\overline{d}$g $\rightarrow t\overline{u}\overline{b}$	$qg \rightarrow tq\overline{b}$
σ [pb]	29.46	13.01	42.47

Table 5: Process 3.1 $bg \rightarrow tW$.

Subprocess	$bg \rightarrow tW$
σ [pb]	56.24

Table 6: Processes 3.2 $q\overline{q} \rightarrow tW\overline{b}$ and 3.3 gg $\rightarrow tW\overline{b}$.

Subprocess	$u\overline{u} \rightarrow tW\overline{b}$	$d\overline{d} \rightarrow tW\overline{b}$	$q\overline{q} \rightarrow tW\overline{b}$	gg $\rightarrow tW\overline{b}$
σ [pb]	2.76	2.73	5.49	19.21

The resulting total cross-section for the single top quarks production is 245.62 pb, which includes the W - gluon fusion mechanism contribution of 159.36 pb, what represents $\sim 65\%$ of the total single top quark rate for all the processes considered.

Above calculations seem to be in reasonable agreement with similar NLO calculations[10] performed rather recently.

In the SM top quarks decay to a W boson and a b quark. In this study we have considered only a W decay to a lepton and neutrino, as this signal should be easier to find experimentally than hadronic decays of the W bosons. The branching ratio for this decay mode is 1/9.

4 Event simulation

The simulation of the signal and corresponding backgrounds processes was performed with the ATLFAST (version 1.62) code[11]. PYTHIA 5.7/JETSET 7.4 was used as event generator[12]. PYTHIA includes the basic W - gluon fusion reaction according to SM assumptions.

An advantage of the W - gluon fusion process is in certain kinematical features of the final state particles. These features could be useful to suppress the background. The study presented here aimed to exploit these features.

A typical W - gluon fusion event is shown in Fig. 2(left). A t - quark decays to $(bl\nu_l)$ via a real W, so a high p_T isolated lepton will appear in the final state accompanied by a number of jets.

There is no exact process for $2 \rightarrow 3$ W - gluon fusion single top quarks production in PYTHIA, therefore a simplified approximation to generate this diagram has been used. In the spirit of the paper[13] the $2 \rightarrow 2$ process with a massive quark in the final state was generated. The additional quark jet needed to provide the required $2 \rightarrow 3$ process has been recovered from PYTHIA partonic shower (see Fig. 2(right)). As it was shown in Ref.[14], such approximation for the kinematics of outgoing quarks are in reasonable agreement with a parton Monte-Carlo where a full matrix element was implemented.

The partonic distribution function set CTEQ2L[16] has been used in the signal and background calculations. The effects of the initial- and final- state radiation, hadronization and multiple interactions of initial partons were included. The value of 175 GeV was assigned to the top quark mass.

In order to reduce the enormous QCD multijet background, as well as provide a high p_T lepton for trigger purposes, we concentrated on the single top production with $t \rightarrow Wb$ followed by a leptonic decay $W \rightarrow l\nu$, where the charged lepton is a positron. As was mentioned in section 2, two main background processes have been considered. The first one is the $t\bar{t}$ pair production, where one W from the top quark decays via leptonic channel, while the second W produces jets. The second background source is the QCD W + jet production, when the W also decays to lepton + neutrino.

The total cross-section values (in pb) which were used in our study are presented in Table 7. Only the W branching to a positron and a neutrino has been considered. As for pre-selection we used the cut Njet≥ 2 for the signal and background processes.

To define an optimal strategy for the top quark selection and the background suppression, the partonic level information has been used. It could be useful to exploit the differences between signal and background reflecting in distributions on various kinematical variables. The partonic spectra in the W - gluon fusion process are presented in Fig. 3.

The transverse momenta of a leading (spectator) quark, a $\bar{b}$ quark and a b quark from the top quark decay are shown in Fig.3(top). The corresponding pseudorapidity distributions are pre-

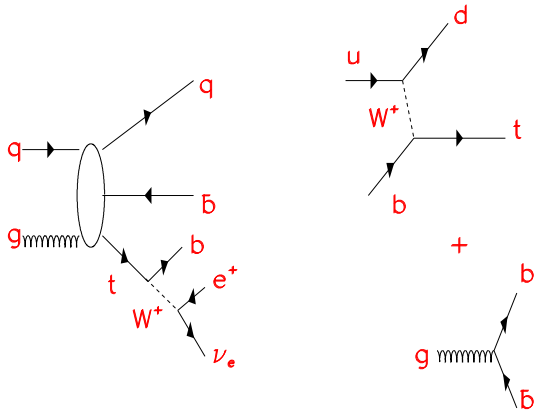

Figure 2: Typical W - gluon fusion event (left) and scheme of the signal simulation (right).

Table 7: Cross sections (in pb) used in this study.

Process type	$Wg \rightarrow t\bar{b}$	$t\bar{t}$	W+jets
σ_{total}	245	833	
$\sigma \times BR$	17	61	23410
σ Njet$\geq$ 2	14	60	2233

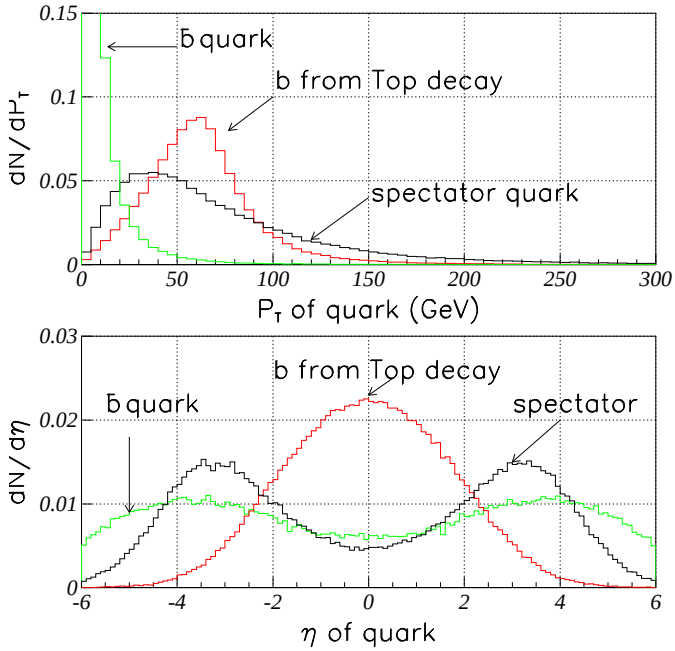

Figure 3: Distributions at partonic level for $\overline{b}$, b from top decay and spectator quark: P_T(top) and η(bottom) variables.

sented in Fig.3(bottom). It can be seen that the spectator quark is produced with high p_T and mainly emitted in the forward direction. This gives the possibility to tag a spectator jet in ATLAS hadronic endcap or forward calorimeters. At the same time the b-quark jet from the top quark decay, also carrying a high transverse momentum is predominantly emitted in the central pseudorapidity region and can be b-tagged. The third jet from a $\overline{b}$ quark has almost a broad pseudorapidity distribution and has a relatively small p_T . Therefore, applying appropriate p_T cuts this jet could be well separated from b-tagged jets produced in top quarks decay.

Fig. 4(a,b) shows that the lepton and ν from the top quark decay are possess a large transverse momentum and emitted in the central pseudorapidity region. Since we have one top quark decay per event in the signal simulation, a good ν reconstruction is required. To perform this reconstruction a missing p_T ($\not{p}_T$) and longitudinal p_z^ν neutrino momenta are needed to calculate.

5 Signal and background selection and event reconstruction

Distributions of the number of reconstructed jets per event in the signal and background processes are plotted in Fig. 5 for the all jets and for the jets originating from a b-quark.

The ATLFAST default parameters for jet cluster reconstruction are the following: $p_T >$ 15 GeV, cone size value ΔR=0.4 in the barrel region, and $\Delta R = 0.7$ in the forward direction ($\eta > 2.5$).

To isolate the W - gluon fusion process under study, the events which contain isolated lepton with $p_T > 30$ GeV and two jets with $p_T > 30$ GeV in the final state have been selected.

To tag the spectator quark, the jet in the forward direction $(\eta > 2.5)$ and $p_T > 50$ GeV has been searched.

The b - jet reconstruction and tagging technique in ATLFAST have been used. A jet cluster was identified as a b-jet if a b - quark of $p_T > 5$ GeV after at the final - state radiation is found in a cone of $\Delta R_{cone} = 0.2$ around the reconstructed jet for jets with $|\eta| < 2.5$.

To have more realistic b-jet tagging efficiencies, the ATLFAST-B package has been used.

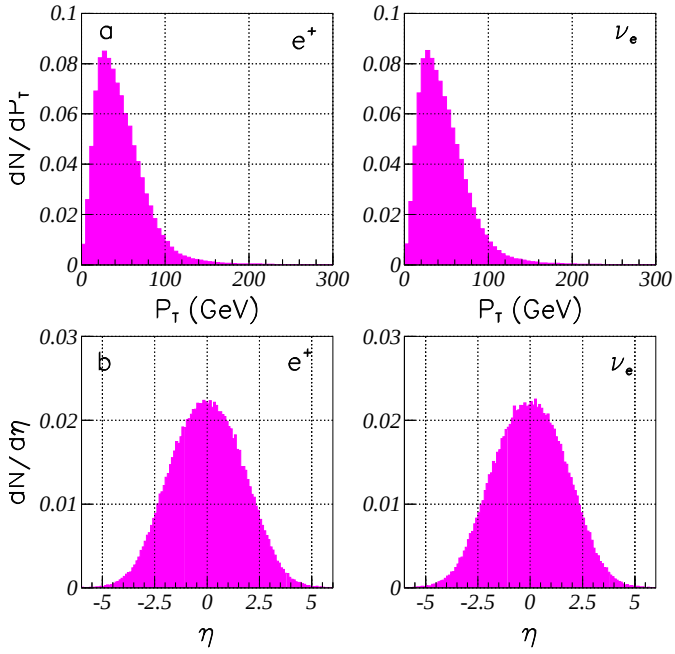

Figure 4: Partonic distributions of P_T(a) and η(b) of electron and neutrino.

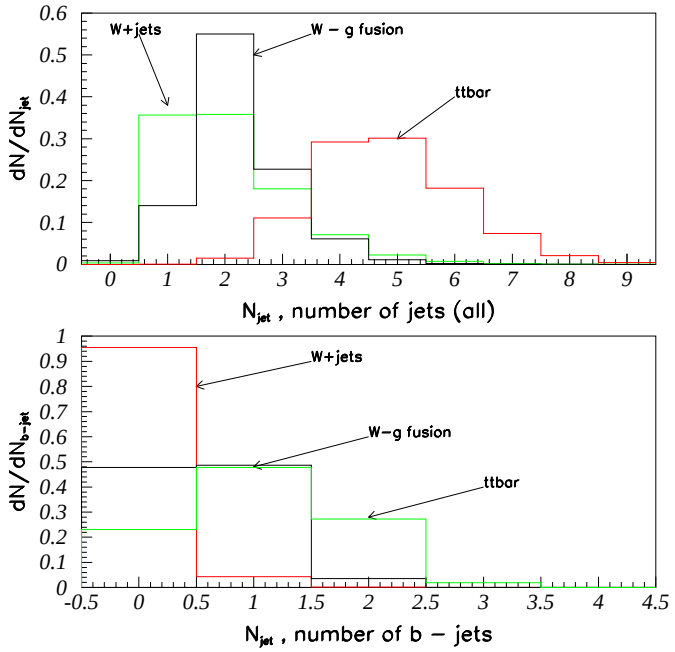

Figure 5: Distributions on the number of all jets and b - jets for the signal and background processes

The efficiency for b jets tagging, ε, of $\sim 63\%$ has been used with the corresponding admixture of mistagged c - jets of 10% and of lights quarks misidentification - 1%.

To separate the W - gluon fusion event, only one identified b - jet in the event was selected.

To identify b - jets from top quarks decay, jet with $p_T > 50$ GeV were selected.

For the reconstruction of the W decay products, the $\not{p}_T$ was computed as a vectorial sum of p_T for all reconstructed particles in the event. In Fig. 6(left) the difference between the computed $\not{p}_T$ and the p_T of the neutrino at partonic level is shown. The $\not{p}_T$ reconstruction is satisfactory.

The longitudinal component of neutrino momentum can be estimated from the $\not{p}_T$ and the lepton momentum from the real W decay using only a constraint on the W mass. The W mass value, $M_W = 80$ GeV, smeared according to it's known width has been used to solve the quadratic equation and a pair of solutions for p_z^ν was obtained.

Two approaches to pick-up a "right" solution from the two available ones were used. In the first one, the minimum between the two absolute values of p_z^ν has been taken to compute the effective mass, $(m_{l\nu jet})$.

Fig. 6(right) shows the difference between the selected minimal $|p_z^\nu|$ value and P_z^ν at partonic level P_z^ν. It can be seen that the longitudinal momentum of neutrino significantly defines the neutrino momentum resolution.

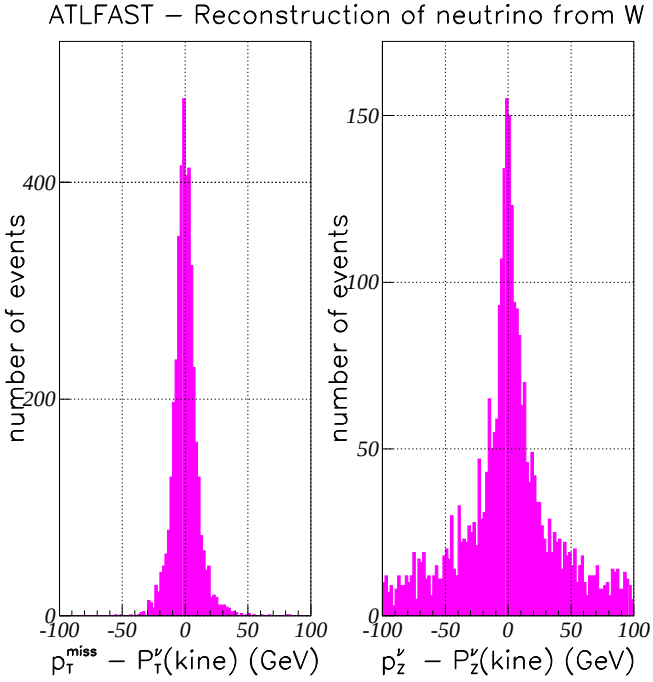

Figure 6: $\not{p}_T$ - P_T^ν (left), $|p_z^\nu|$ - $|P_z^\nu|$ (right)

In the second approach, both solutions in absolute value were taken to compute $(m_{l\nu jet})$, then the solution nearest to the "known" M_{top} value used. This was done with the aim to obtain conditions for a better cross-section measurement rather than to improve the accuracy of the single top quark mass reconstruction.

The same cuts as for the signal data set were applied for background events.

The simulation of W + jets to accumulate statistics for high values of the $(m_{l\nu jet})$ mass was performed in different regions of $\hat{P}_t$ and then normalized and summed. W + jets data sample consists of W plus at least 2 jets, where for the jets any of the quark flavour available has been allowed. No other special kinematical cuts at the generation stage have been applied.

To suppress background events effectively, cuts on different kinematic variables could be

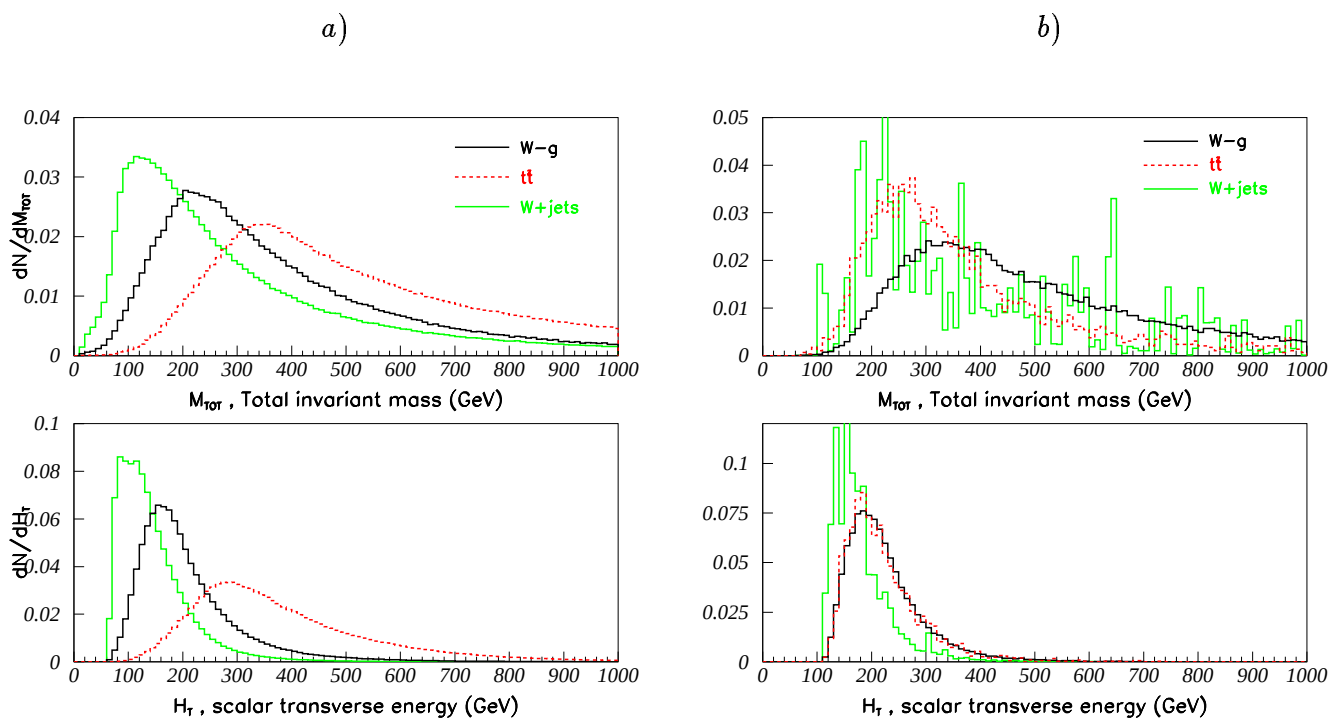

Figure 7: Total event invariant mass, M_{tot} (top) and scalar transverse energy, H_T (bottom) for W-gluon fusion (signal), $t\bar{t}$ and W+jets events (background). Distributions shown before (a) and after cuts (b), respectively.

useful. This strategy is based on differences in corresponding distributions for signal and background (see Ref.[18], for example).

Fig. 7(top) shows the total event invariant mass, recostructed from the 4-vectors of all of the jets and leptons found in the event. A significance difference is observed between the invariant mass of events in the non-top backgrounds and the signal.

Another variable of interest is the scalar sum of transverse momenta of jets and lepton, $H_T = |E_T^{jet_1}| + |E_T^{jet_2}| + |E_T^{lepton}|$ used in this study. Distributions of H_T for signal events and background are shown in Fig. 7(bottom). As one can see, it is possible to select events in a range of kinematic variables presented (or a combination of them), where the contribution of signal events would dominate. Distributions shown before all previous cuts, Fig. 7a), and after cuts, Fig. 7b), respectively. To suppress $t\bar{t}$ and W+jets background events, we put cuts on the H_T variable of $H_T > 200$ GeV and $M_{tot} > 300$ GeV, correspondigly.

Used cuts and resulting efficiencies are given in the Table 8. The last line of Table shows the number of events survived cuts.

Resulting reconstructed mass of the $(l\nu jet)$ system for the signal and background events is presented in Fig. 8. Results are shown for 3 years ATLAS running at low luminosity ($3 \times 10^4 pb^{-1}$).

Finally, a good signal (S) and background (B) separation prediction has been achieved: $S/B \sim 4.9$ (estimated for production of both types of the top quark), and $S/\sqrt{B}$ = 286. From Table 8 the fractional uncertainty in the cross section ($\sqrt{(S+B)}/S$) is 0.84%. This lead to a relative error on V_{tb} of 0.42%.

Table 8: Effective cuts used to optimize the W-gluon fusion signal. Efficiencies for cumulative effect of cuts are shown. Only events with the number of jets ≥ 2 are included.

Type of events	$Wg \to t\bar{b}$	$t\bar{t}$ pairs	W+jets
Number of events $L = 3 \times 10^4 pb^{-1}$	347372	1.8×10^6	6.7×10^7
	Efficiency (%)	Efficiency (%)	Efficiency (%)
Cuts used:			
1 lep + 1 b-jet	26.8	57.87	0.32
Njets=2	16.7	2.98	0.15
Leading quark tag	6.95	0.19	2.7×10^{-2}
$H_T > 200$ GeV	3.92	0.10	7.1×10^{-3}
$M_{tot} > 300$ GeV	3.58	0.08	5.7×10^{-3}
150 GeV$< M_{top} <$200 GeV	3.21	0.04	2.0×10^{-3}
Events after cuts	11148	734	1295

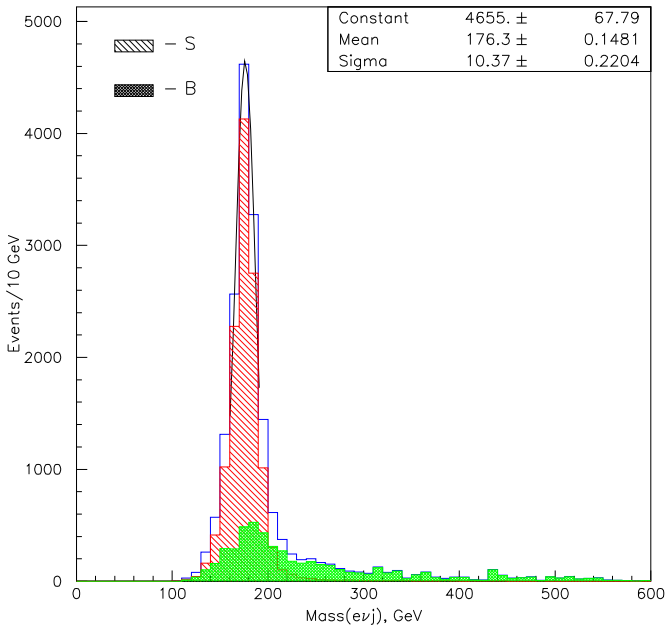

Figure 8: Reconstructed mass for $l\nu jet$ system

6 Conclusions

The single top quark production via W - gluon fusion at $\sqrt{s} = 14$ TeV has been investigated. Simulation for the signal and background was performed with ATLFAST and PYTHIA 5.7/JETSET 7.4 packages. The difference between the signal and background, identified with various kinematical distributions, allow to suppress the backgrounds rather well. The stream of cuts to optimize the signal-to-background ratio has been presented. On the basis of the applied cuts it is possible to estimate the S/B ratio and the error on the cross-section measurement in the W-gluon channel. Taking into account the production of both types of top quark, the ratio $S/B \sim 4.9$ has been obtained, and the precision on the cross-section measurement equal to $\delta(V_{tb})/V_{tb}$=0.42%.

While the obtained values for S/B and $\delta(V_{tb})/V_{tb}$ are in rather good agreement with the numbers presented in the TDR, one can notice that the rejection of W+jets PYTHIA events in our study is somewhat better than the numbers provided in the TDR for W+jets events generated by HERWIG event generator. To understand the origin of this difference the comparison of PYTHIA and HERWIG event generators will be presented our next Note (in preparation), in which different leptonic decays of W from top quarks decay will be analysed separately, as well.

7 Acknowledgment

We would like to thank C.Brock, M.Cobal, B.Gonzales-Pineiro, Y.Gouz, D. O'Neil, J.Parsons, E.Richter-Was, T.Sjostrand, S.Slabospitsky for many valuable discussions during the preparation of this work.

References

[1] S.Abachi et al. (D0 Collab.), *Phys.Rev.Lett.*, **74** (1995), p.2632
[2] F.Abe et al. (CDF Collab.), *Phys.Rev.Lett.*, **74** (1995), p.2626
[3] E.Eichten and K.Lane, *Phys.Lett.* **B327**,(1994), p.129;
T.Appelquist and G.Tryantaphyllou, Phys.Rev.Lett. **69**, (1992), p.2750;
G.Liu et al, *Phys.Rev.* **D54**, (1996), p.1083;
[4] O.Cakır and M.Yilmaz, *Europhys.Lett.*, **41**, (1998), p.257
[5] G.Kane et al., *Phys.Rev.* **D45**, (1992), p.124;
T.Han et al., *Phys.Lett.* **B385**, (1996), p.311;
T.Han et al., *Phys.Rev.* **D55**, (1997), p.7241;
M.Felcini. Proc. of LHC Workshop, Aachen, Germany, 1990. Vol.2, p.414.
[6] E.Eichten, I.Hichliffe, K.Lane and C.Quigg, *Rev.Mod.Phys.* **56**, (1984), p.579; **58**, (1986), p.1065, *Phys.Rev.* **D34**, (1986), p.1547
[7] S.Weinberg, *Phys.Rev.* **D19**, (1979), p.1277; L.Susskind, *ibid.*, **D20**, (1979), p.2619
[8] B.Holdom, *Phys.Rev.* **D24**, (1981), p.1441;
T.Appelquist, L.C.R.Wijewardhana, *Phys.Rev.* **D35**, (1987), p.774;
T.Akiba and T.Yanagida, *ibid.*, **B169**, (1986), p.432
[9] Blondel A., *Proc. of the 28th Int. Conf. on High Energy Phys. (ICHEP'96)* (Warsaw, Poland) 1996, p.205
[10] T.M.Tait, *Phys.Rev.***D61**, 034001 (2000);
T.Stelzer,Z.Sullivan and S.Willenbrock,*Phys.Rev.***D56**, 5919 (1997)
M.C.Smith and S.Willenbrock,*Phys.Rev.***D54**, 6696 (1996)
[11] ATLFAST 2.0, ATLAS Internal Note, ATL-PHYS-98-131, CERN (1998)
[12] T.Sjostrand, *Computer Physics Commun.*, 82, (1994), p.74

[13] G.Unal, L.Fayard, Large Hadron Collider Workshop, Aachen, 1990
[14] T.Moers et al., Large Hadron Collider Workshop, Aachen, 1990
[15] ATLAS Collaboration, “ATLAS Calorimeter Performance. Tecnical Design Report”, CERN/LHCC/96-40, ATLAS TDR1(1996)
[16] H.L.Lai et al., *Phys.Rev.*, **D**51 ,(1995), p.4763
[17] G.Bordes and B.van Eijk, *Nucl.Phys.*, **B**435, (1995), p.23
[18] S.Willenbrock and D.Dicus, *Phys.Rev.* **D**34, (1986) p.155;
C.P.Yuan, *ibid.* 41, (1990), p.42;
D.Amidei et al., Top physics and the Tevatron,
CDF/DOC/TOP/PUBLIC,(1995) (unpublished), p.3265;
G.V.Jikia and S.R.Slabospitsky *Phys.Lett.* **B**295 (1992) p.136
[19] A.Heinson, A.Belyaev, and E.Boos, INP-MSU-96-11/448, UCS 196-25, hep-ph/9612424, 1996; A.Belyaev, E.Boos, L.Dudko, hep-ph/9804328, 1998.
[20] C.Sachrajda, *Phys.Lett.* **B**73, (1978), p.185 and ibid. **B**76, (1978), p.100;
R.K.Ellis, H.Georgi, M.Machacek, H.D.Politzer and G.C.Roos, *Phys.Lett.*, **B**78, (1987), p281.
[21] ATLAS Detector and Physics Performance Technical Design Report CERN/LHCC/99-15, Volume 2.